Analytical relationships for re-entrant honeycombs

R. Hedayati[1*], N. Ghavidelnia[2]

[1]Novel Aerospace Materials Group, Faculty of Aerospace Engineering, Delft University of Technology (TU Delft), Kluyverweg 1, 2629 HS Delft, the Netherlands

[2]Department of Mechanical Engineering, Amirkabir University of Technology (Tehran Polytechnic), Hafez Ave, Tehran, Iran

---

[1] Corresponding author, email addresses: r.hedayati@tudelft.nl, rezahedayati@gmail.com, Tel: +31 (0)15 27 88777

Abstract

Mechanical metamaterials have emerged in the last few years as a new type of artificial material which show properties not usually found in nature. Such unprecedented properties include negative stiffness, negative Poisson's ratio, negative compressibility and fluid-like behaviors. Unlike normal materials, materials with negative Poisson's ratio (NPR), also known as auxetics, shrink laterally when a compressive load is applied to them. The 2D re-entrant honeycombs are the most prevalent auxetic structures and many studies have been dedicated to study their stiffness, large deformation behavior, and shear properties. Analytical solutions provide inexpensive and quick means to predict the behavior of 2D re-entrant structures. There have been several studies in the literature dedicated to deriving analytical relationships for hexagonal honeycomb structures where the internal angle θ is positive (i.e. when the structure has positive Poisson's ratio). It is usually assumed that such solutions also work for corresponding re-entrant unit cells. The goal of this study was to find out whether or not the analytical relationships obtained in the literature for $\theta > 0$ are also applicable to 2D-reentrant structures (i.e. when $\theta < 0$). Therefore, this study focused on unit cells with a wide range of internal angles from very negative to very positive values. For this aim, new analytical relationships were obtained for hexagonal honeycombs with possible negativity in the internal angle θ in mind. Numerical analyses based on finite element (FE) method were also implemented to validate and evaluate the analytical solutions. The results showed that, as compared to analytical formulas presented in the literature, the analytical solutions derived in this work give the most accurate results for elastic modulus, Poisson's ratio, and yield stress. Moreover, some of the formulas for yield stress available in the literature fail to be valid for negative ranges of internal angle (i.e. for auxetics). However, the yield stress results of the current study demonstrated good overlapping with numerical results in both the negative and positive domains of θ.

Keywords: NPR; auxetics; analytical; re-entrant; Poisson's ratio; honeycombs.

1. Introduction

Metamaterials have emerged in the last few decades as a new type of artificial material which show physical properties not usually found in nature [1, 2]. Mechanical metamaterials are new category of metamaterials which exhibit unprecedented properties such as negative stiffness, negative Poisson's ratio [3, 4], negative compressibility [2, 5] and fluid-like behaviors [6, 7]. Unlike normal materials, materials with negative Poisson's ratio (NPR), also known as auxetics, shrink laterally when a compressive load is applied to them. Auxetics have found many applications in novel products as they offer high energy absorption capacity, high indentation resistance, and fracture toughness [5]. Their special ability to deform differently in the transverse direction also makes them suitable to be used as building blocks in actuators [8-10].

There are several types of designer auxetics including re-entrant [11, 12], rotating semi-rigid structures [13, 14], chiral [15-17], and origami-based [18, 19] auxetics. The 2D re-entrant honeycombs (Figure 1c) are the most prevalent auxetic structures and many studies have been dedicated to study their stiffness [20], large deformation behavior [21], and shear properties [22] using analytical, numerical, and experimental approaches. Analytical solutions provide inexpensive and quick means to predict the behavior of 2D re-entrant structures [23].

There have been several studies [24-26] dedicated to deriving analytical relationships for hexagonal honeycomb structures where the internal angle θ is positive (See Figure 1b). It is usually assumed that such solutions also work for corresponding re-entrant unit cells (See Figure 1c). The goal of this study is to find out if the analytical relationships obtained in the literature for $\theta > 0$ are also applicable to 2D-reentrant structures. Therefore, this study focuses on unit cells with a wide range of internal angles from very negative to very positive. For this aim, analytical relationships have been obtained for hexagonal honeycombs with possible negativity in the internal angle θ in mind (i.e. 2D re-entrant unit cells). Numerical analyses based on finite element (FE) method have been implemented to validate and evaluate the analytical solutions.
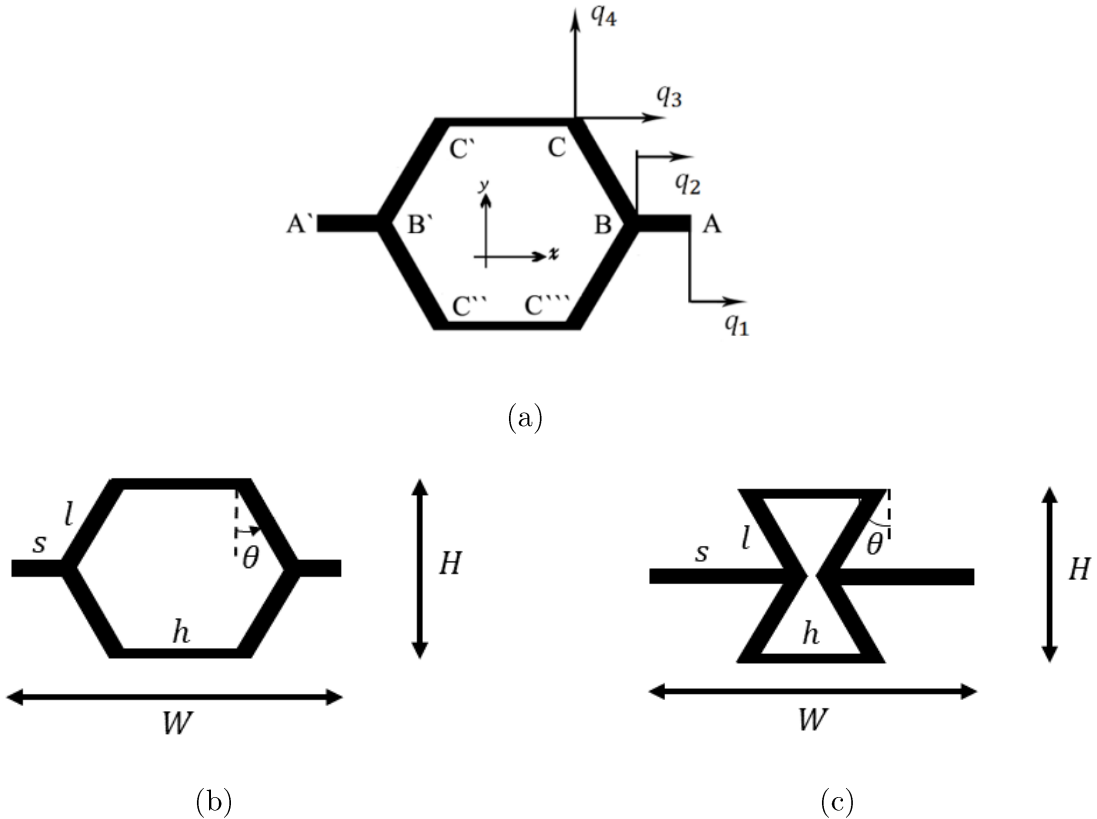
Figure 1: (a) DOFs of a unit cell, and (b,c) dimensions of hexagonal and re-entrant unit cells

2. Materials and Methods

2.1. Stiffness matrix

The method used here for obtaining the elastic properties is very similar to what is presented in [24]. As the way the cells are organized and their center-to-center distance is different from [24], there are some minor differences in derivations. Therefore, the full procedure of obtaining the elements of the stiffness matrix is not presented in the main paper, but it is provided in the Appendix accompanying the paper.

The external forces required to be applied to a degree of freedom q_i is denoted by Q_i. The force-displacement relationship of this system has the following form:

$$\begin{Bmatrix} Q_1 \\ Q_2 \\ Q_3 \\ Q_4 \end{Bmatrix} = \begin{bmatrix} k_{11} & k_{12} & k_{13} & k_{14} \\ k_{21} & k_{22} & k_{23} & k_{24} \\ k_{31} & k_{32} & k_{33} & k_{34} \\ k_{41} & k_{42} & k_{43} & k_{44} \end{bmatrix} \begin{Bmatrix} q_1 \\ q_2 \\ q_3 \\ q_4 \end{Bmatrix} \tag{1}$$

where the stiffness matrix elements k_{ij} must be determined in order to obtain the displacements, rotations, forces and moments as a function of the applied force F from which different elastic properties of a unit cell can be found. By looking at the geometries in Figure 1, it can be seen that $s = \frac{1}{2}(W - H\tan\theta - h)$ and $l = \frac{H}{2\cos\theta}$.

Using the obtained stiffness matrix elements (see Appendix), the force-displacement relationships using the stiffness matrix can be constructed as

$$\begin{Bmatrix} Q_1 \\ Q_2 \\ Q_3 \\ Q_4 \end{Bmatrix} = \begin{bmatrix} \frac{2AE}{s} & -\frac{2AE_s}{s} & 0 & 0 \\ -\frac{2AE}{s} & \frac{4AE_s}{l}\sin^2\theta + \frac{48E_sI}{l^3}\cos^2\theta + \frac{2AE_s}{s} & -\frac{4AE_s}{l}\sin^2\theta - \frac{48E_sI}{l^3}\cos^2\theta & \left(\frac{4AE_s}{l} - \frac{48E_sI}{l^3}\right)\cos\theta\sin\theta \\ 0 & -\frac{4AE_s}{l}\sin^2\theta - \frac{48E_sI}{l^3}\cos^2\theta & \frac{48E_sI}{l^3}\cos^2\theta + \frac{4AE_s}{l}\sin^2\theta + \frac{4AE_s}{h} & \left(\frac{48E_sI}{l^3} - \frac{4AE_s}{l}\right)\cos\theta\sin\theta \\ 0 & \left(\frac{4AE_s}{l} - \frac{48E_sI}{l^3}\right)\sin\theta\cos\theta & \left(\frac{48E_sI}{l^3} - \frac{4AE_s}{l}\right)\cos\theta\sin\theta & \frac{4AE_s}{l}\cos^2\theta + \frac{48E_sI}{l^3}\sin^2\theta \end{bmatrix} \begin{Bmatrix} q_1 \\ q_2 \\ q_3 \\ q_4 \end{Bmatrix} \tag{2}$$

The corresponding force-displacement relationship for Timoshenko beam theory can be obtained by replacing $\frac{12E_sI}{l^3}$ in the Euler-Bernoulli equation by $\frac{1}{\frac{12E_sI}{l^3} + \frac{l}{2\kappa AG_s}}$ which yields

$$\begin{Bmatrix} Q_1 \\ Q_2 \\ Q_3 \\ Q_4 \end{Bmatrix} = \begin{bmatrix} \frac{2AE_s}{s} & -\frac{2AE}{s} & 0 & 0 \\ -\frac{2AE_s}{s} & \frac{4AE_s}{l}\sin^2\theta + \frac{4}{\frac{l^3}{12E_sI} + \frac{l}{2\kappa AG_s}}\cos^2\theta + \frac{2AE_s}{s} & -\frac{4AE_s}{l}\sin^2\theta - \frac{4}{\frac{l^3}{12E_sI} + \frac{l}{2\kappa AG_s}}\cos^2\theta & \left(\frac{4AE_s}{l} - \frac{4}{\frac{l^3}{12E_sI} + \frac{l}{2\kappa AG_s}}\right)\cos\theta\sin\theta \\ 0 & -\frac{4AE_s}{l}\sin^2\theta - \frac{4}{\frac{l^3}{12E_sI} + \frac{l}{2\kappa AG_s}}\cos^2\theta & \frac{4}{\frac{l^3}{12E_sI} + \frac{l}{2\kappa AG_s}}\cos^2\theta + \frac{4AE_s}{l}\sin^2\theta + \frac{4AE_s}{h} & \left(\frac{4}{\frac{l^3}{12E_sI} + \frac{l}{2\kappa AG_s}} - \frac{4AE_s}{l}\right)\cos\theta\sin\theta \\ 0 & \left(\frac{4AE_s}{l} - \frac{4}{\frac{l^3}{12E_sI} + \frac{l}{2\kappa AG_s}}\right)\sin\theta\cos\theta & \left(\frac{4}{\frac{l^3}{12E_sI} + \frac{l}{2\kappa AG_s}} - \frac{4AE_s}{l}\right)\cos\theta\sin\theta & \frac{4AE_s}{l}\cos^2\theta + \frac{4}{\frac{l^3}{12E_sI} + \frac{l}{2\kappa AG_s}}\sin^2\theta \end{bmatrix} \begin{Bmatrix} q_1 \\ q_2 \\ q_3 \\ q_4 \end{Bmatrix} \tag{3}$$

The external forces acting on vertex B is zero, and the external force acting on point C in the X direction is zero, thus $Q_2 = Q_3 = 0$. On the other hand, the force acting on point C in the Y direction is $\sigma_y bW$, and the external force acting on point A is $\sigma_x bH$. Then, the force vector becomes

$$\begin{Bmatrix} Q_1 \\ Q_2 \\ Q_3 \\ Q_4 \end{Bmatrix} = \begin{Bmatrix} \sigma_x \, bH \\ 0 \\ 0 \\ \sigma_y \, bW \end{Bmatrix} \qquad (4)$$

2.2 Obtained mechanical properties

The unknown elements can be obtained simply by inverting the stiffness matrix given in Eq. (2) or (3) and by multiplying it in the force vector given in Eq. (4). Using the obtained unknowns q_i, it is possible to calculate the elastic modulus, Poisson's ratio, and yield stress as a function of the geometrical and material properties E_s, σ_{y_s}, and ν_s. In all the following derivations, the formulas $s = \frac{1}{2}(W - H\tan\theta - h)$ and $l = \frac{H}{2\cos\theta}$ are considered.

a) Elastic Modulus

The elastic modulus in each direction is found by dividing stress in that direction (i.e. $\sigma_x \, W/2q_1$ in the X direction and $\sigma_y H/2q_4$ in the Y direction) into strain in that direction,. Using the Euler-Bernoulli stiffness matrix, the relative elastic modulus in the X direction is obtained as (σ_y=0):

$$\left(\frac{E}{E_s}\right)_X = \frac{Wt^3 cos\theta}{H\{l\,(l^2-t^2)\cos^3\theta + t^2(l+W)cos\theta - Ht^2 sin\theta\}} \qquad (5)$$

and using the Timoshenko stiffness matrix, the relative elastic modulus in the X direction is obtained as

$$\left(\frac{E}{E_s}\right)_X = \frac{5Wt^3 cos\theta}{H\{l(5l^2 + 7t^2 + 11t^2\nu_s)\cos^3\theta + 5t^2(l+W)cos\theta - 5Ht^2 sin\theta\}} \qquad (6)$$

Using the Euler-Bernoulli stiffness matrix, the relative elastic modulus in the Y direction is obtained as

$$\left(\frac{E}{E_s}\right)_Y = \frac{Ht^3}{Wl\{(l^2 - t^2)\,sin^2\,\theta + t^2\}} \qquad (7)$$

and using the Timoshenko stiffness matrix, the relative elastic modulus in the Y direction is obtained as

$$\left(\frac{E}{E_s}\right)_Y = \frac{5Ht^3}{Wl\{(5l^2 + 7t^2 + 11t^2v)\sin^2\theta + 5t^2\}} \tag{8}$$

b) Poisson's ratio

The Poisson's ratio can be obtained by dividing the two strains in X and Y directions. For v_{xy}, we have $v_{xy} = -\frac{\varepsilon_y}{\varepsilon_x} = \frac{q_2}{q_1}\frac{W}{H}$ for $\sigma_y = 0$. Using the Euler-Bernoulli force-displacement relationship, the Poisson's ratio v_{12} is found as

$$v_{xy} = \frac{Wl\cos^2\theta\,\sin\theta(l^2 - t^2)}{H\{l(l^2 - t^2)\cos^3\theta + t^2(l + W)\cos\theta - Ht^2\sin\theta\}} \tag{9}$$

and for Timoshenko beam theory, it becomes

$$v_{xy} = \frac{Wl\cos^2\theta\,\sin\theta(5l^2 + 11vt^2 + 7t^2)}{H\{l(5l^2 + 7t^2 + 11t^2v)\cos^3\theta + 5t^2(l + W)\cos\theta - 5Ht^2\sin\theta\}} \tag{10}$$

For v_{yx}, we have $v_{yx} = -\frac{\varepsilon_x}{\varepsilon_y} = \frac{q_1}{q_4}\frac{H}{W}$ for $\sigma_x = 0$ which for Euler-Bernoulli beam theory gives

$$v_{yx} = \frac{H(l^2 - t^2)\sin(2\theta)}{2W\{(l^2 - t^2)\sin^2\theta + t^2\}} \tag{11}$$

and for Timoshenko beam theory, it becomes

$$v_{yx} = \frac{H(5l^2 + 11v_st^2 + 7t^2)\sin(2\theta)}{W(11v_st^2 + 5l^2 + 17t^2 - (5l^2 + 7t^2 + 11v_st^2)\cos(2\theta))} \tag{12}$$

c) Yield stress

It was seen in the honeycomb unit cell in which loading is applied in X_1 direction, in X_2 direction, and bi-axially that the end points of the inclined edges BC are the location with maximum stress. If the point B is dislocated for q_2 in X_2 direction, and the point C is dislocated for q_4 and q_3 in X_1 and X_2 directions respectively, by assuming that the beam BC is clamped at one of its ends B or C, increase in the axial direction of the beam BC is $q_4\sin\theta + (q_2 - q_3)\cos\theta$. Similarly the lateral displacement of the free end of the beam BC is $(q_2 - q_3)\sin\theta - q_4\cos\theta$. These displacements cause the axial load and bending moments

$$P = \frac{AE_s}{l}(q_4 \sin\theta + (q_2 - q_3)\cos\theta) \tag{13}$$

$$M = \frac{6E_s I}{l^2}((q_2 - q_3)\sin\theta - q_4 \cos\theta)$$

which impose the axial and flexural stresses of

$$\sigma_{axial} = \frac{E_s}{l}(q_4 \sin\theta + (q_2 - q_3)\cos\theta) \tag{14}$$

$$\sigma_{flexure} = \frac{3E_s a}{l^2}((q_2 - q_3)\sin\theta - q_4 \cos\theta)$$

By adding the axial and flexural stress in the above equation, the maximum stress in the honeycomb unit cell can be found as $\sigma_{max} = |\sigma_{axial}| + |\sigma_{flexure}|$. The yield stress of the structure can then be found by

$$\sigma_{pl} = \frac{\sigma_{ys}\sigma_i}{\sigma_{max}} \tag{15}$$

where σ_{ys} is the yield stress of the constructing material and σ_i is the applied stress in direction i. The relative yield stress based on Euler-Bernoulli beam theory in the X direction was found as

$$\left(\frac{\sigma_y}{\sigma_{ys}}\right)_X = \frac{2t^2}{H(3l|cos(\theta)| + t|sin(\theta)|)} \tag{16}$$

and for the Timoshenko beam theory was obtained as

$$\left(\frac{\sigma_y}{\sigma_{ys}}\right)_X = \frac{10lt^2}{H(3|(11v_s t^2 + 5l^2 + 12t^2)cos(\theta)| + 5lt|sin(\theta)|)} \tag{17}$$

The relative yield stress in the Y direction and for Euler-Bernoulli beam theory was found as

$$\left(\frac{\sigma_y}{\sigma_{ys}}\right)_Y = \frac{2t^2}{W(t|cos(\theta)| + 3l|sin(\theta)|)} \tag{18}$$

and for the Timoshenko beam theory was obtained as

$$\left(\frac{\sigma_y}{\sigma_{ys}}\right)_Y = \frac{10lt^2}{W(5lt|\cos(\theta)| + 3|(11v_s t^2 + 5l^2 + 12t^2)\sin(\theta)|)} \tag{19}$$

d) Buckling

Using the classic Euler's buckling theory, the critical elastic buckling force of the critical strut can be found. In the X direction, strut BB` (B` represents the vertex from the neighboring unit cell connected to vertex B) is the critical strut, and it can be considered as a column with two fixed ends under compression (K=0.5). Therefore:

$$P_{cr,AB} = \frac{\pi^2 E_s I_{BB`}}{(Kl_{BB`})^2} = \frac{\pi^2 E_s I}{s^2} \tag{20}$$

Therefore, the critical stress in the X direction is

$$\sigma_{cr} = \frac{P_{cr,AB}}{A_{uc}} = \frac{\pi^2 E_s I}{Hbs^2} = \frac{\pi^2 E_s t^3}{12Hs^2} \tag{21}$$

In the Y direction, strut BC is the critical strut. For strut BC we have (K=1):

$$P_{cr,BC} = \frac{\pi^2 E_s I}{(Kl_{BC})^2} = \frac{\pi^2 E_s I}{l^2} \tag{22}$$

On the other hand, we have $P_{cr,UC} = 2P_{cr,BC} \cos\theta$. As a result, $P_{cr,UC} = 2\frac{\pi^2 E_s I}{l^2}\cos\theta$. The critical stress in the Y direction can then be found as:

$$\sigma_{cr} = 2\frac{\pi^2 E_s I}{l^2 A_{uc}}\cos\theta = \frac{\pi^2 E_s t^3}{6l^2 W}\cos\theta \tag{23}$$

2.3. Numerical modelling

FE simulations were implemented for evaluation and validation of the derived analytical relationships for 2D re-entrant structure. A single unit cell with periodic boundary conditions was considered for this purpose. To obtain the numerical results for mechanical properties of the structure in two main directions, two distinct loading conditions were applied in the x and y directions. To obtain more precise and accurate results, beam elements based on Timoshenko beam theory (BEAM 189, ANSYS APDL) were used for discretization of the struts, and each strut was divided into five Timoshenko beam

elements. As compared to Euler-Bernoulli beam theory, the Timoshenko beam theory, as it takes the transverse shear deformation into account, could result in better prediction of deformation especially in thick beams (i.e. in high values of relative densities). Since the material properties of the bulk material have negligible effect on the normalized material properties of the lattice structure, the linear elastic behavior with the values of $E_s = 200$ GPa and $v_s = 0.4$ were considered for the elastic modulus and Poisson's ratio of the constituent material, respectively. To obtain the numerical results for various values of θ, an APDL script was developed to reduce the analysis time cost. The problem was solved for θ in the range of $-45°$ to $+45°$ to observe the trend of changes in the mechanical properties by gradually going from honeycomb structure to re-entrant structure. It is worth noting that to avoid the rigid body motions, one of the nodes of the unit cells was considered as fully constraint in the ANSYS APDL solver. As the unit cells in the lattice structure were considered to be rigidly connected to each other at the vertices of the structure, the external sides of the unit cells were constrained rotationally as well. The following geometrical properties were considered for the simulations: $W = 0.014$ m, $H = 0.00667$ m, $b = 0.004$ m, and $t = 0.0008$ m.

3. Results and discussions

First, the results of the current study are compared to the results of the previous studies [24-26] which requires to take $s = h/2$. The curves of elastic modulus obtained in this study were higher than the curves based on formula derived by Masters and Evans [26], and they were lower than the curves based on formulas of Gibson and Ashby [25] and Hedayati et al. [24] (Figure 2a,b). While the E_x curves had a domical shape, the E_y curves had bell shape. In general, the elastic modulus obtained in this study were close to the corresponding values in the works of Masters and Evans [26] and Hedayati et al. [24], while they were quite far from the results of Gibson and Ashby [25], see Figure 2a,b. The Gibson and Ashby's [25] formula also predicted infinite value for E_y at $\theta = 0$ (Figure 2b) which is very unrealistic. In a previous study of ours [24], it was shown that the Gibson and Ashby's [25] formulas take some simplifying assumptions which makes them only suitable for very thin (paper or metal-sheet) honeycombs. However, as for the case of thick honeycombs, which are most the times the only feasible options in the AM honeycombs, the Gibson and Ashby's [25] formulas deviate from the experimental and numerical results.

As for the Poisson's ratio (Figure 2c-d), all the curves had good overlapping with one another, except for the case of the Gibson and Ashby's [25] formulas. The Gibson and Ashby's [25] formula gave non-realistic extreme values for Poisson's ratio v_{yx} when θ approached zero. All the curves had symmetry with respect to the origin of the plot (i.e. θ=0 and $v_{yx} = 0$).

As for the yield stress, the formulas proposed by other works failed to give correct answers in $\theta < 0$ (they are shown by dashed gray curves in Figure 2e-f), even though those works had not claimed that their formulas is also applicable to negative ranges of θ. The yield stress results of the current study, demonstrated good overlapping with numerical results in both the negative and positive domains of θ. The yield stress values were symmetrical with respect to the line $\theta = 0$ (Figure 2e-f). While the yield stress in the y direction had a noticeable peak at $\theta = 0$, the curves for the yield stress in the x direction were relatively independent from the internal angle θ.

Even though the results presented in Figure 2 demonstrated the validity of our analytical solution, they are presented for a constant $\frac{s}{h} = 1/2$ ratio. They were plotted for a constant s/h ratio of $1/2$, because this assumption has been considered in the previous studies [24-26] where analytical solutions for hexagonal honeycombs are derived. In many actual metamaterials, such as gradient [8] and random [27] auxetic metamaterials, the ratio s/h should vary throughout the structure to keep the width W and height H of all the unit cells equal. See for example the unit cells presented in Figure 1b and Figure 1c which have the same width W and height H. The trends of the graphs presented for variable s/h ratio (Figure 3) are in general similar to what was observed for constant s/h ratio of $1/2$ (Figure 2). As compared to the results of the case with constant s/h ratio of 1/2, the values obtained for the case of variable s/h is in general lower (with a maximum difference of 0.59% in the x direction and 0.38% in the y direction), lower (with a maximum difference of 0.077% for xy and 0.036% for yx), and equal values for respectively elastic modulus, Poisson's ratio, and yield strength. It is also beneficial to note that the Timoshenko and Euler-Bernoulli results are very similar to one another in all the cases other than in E_x and σ_x. They have a maximum difference of 13.23%, 9.66%, 2.61%, 8.96%, 14.18%, and 11.96% for respectively E_x, E_y, v_{xy}, v_{yx}, σ_x, and σ_y.
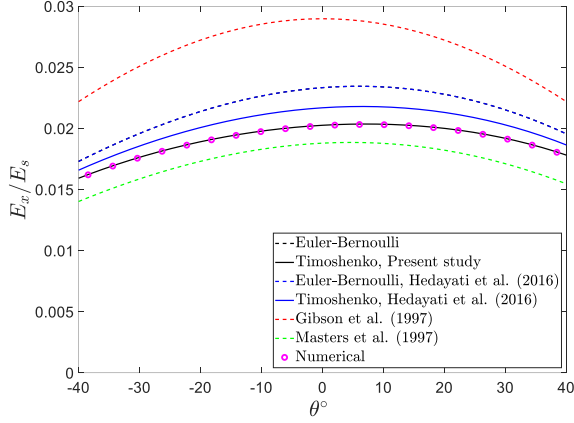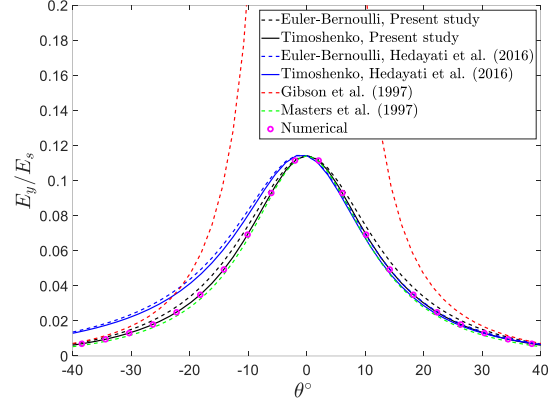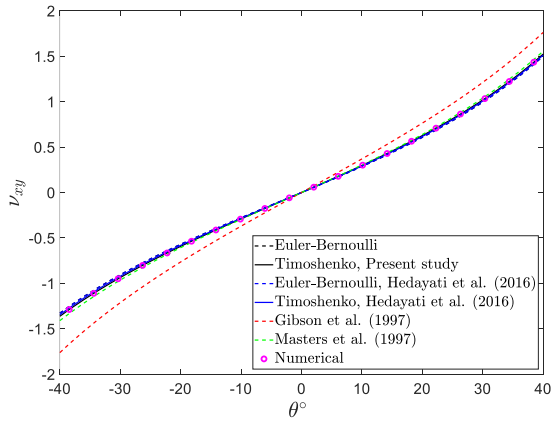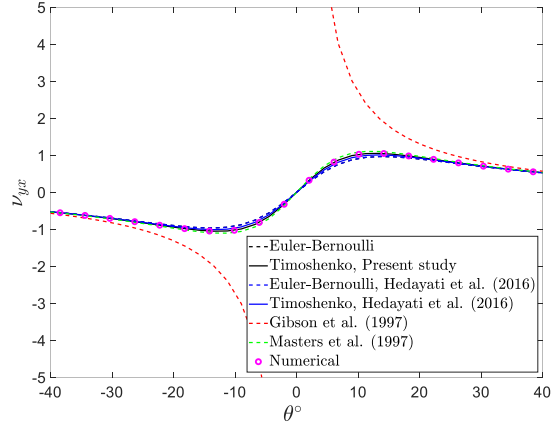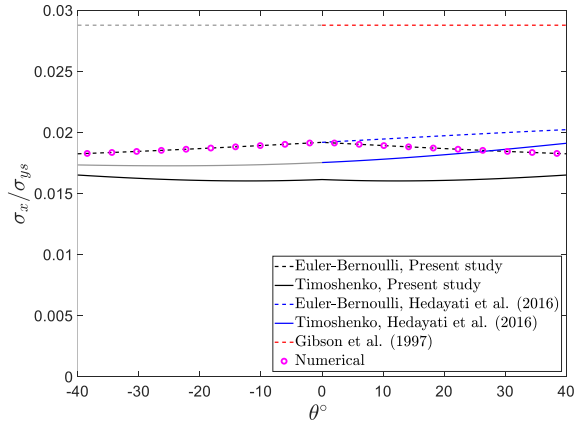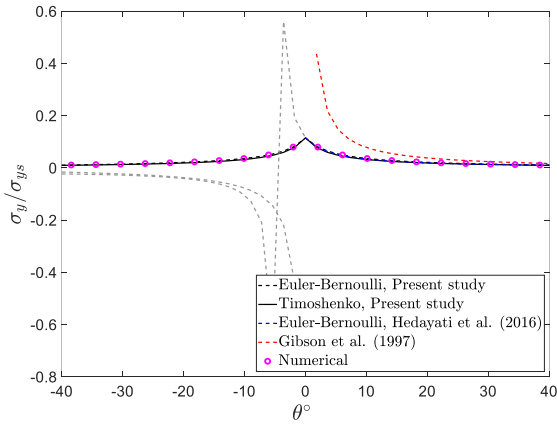
Figure 2: Comparison of (a) E_x, (b) E_y, (c) ν_{xy}, (d) ν_{yx}, (e) σ_x, and (f) σ_y between the results of the current study and previous studies for $s = h/2$. The yield strength formulas in Hedayati et al [24] and Gibson et al [25] are obtained for $\theta > 0$. The extension of curves attributed to those formulas to $\theta < 0$ is therefore demonstrated by grey color.
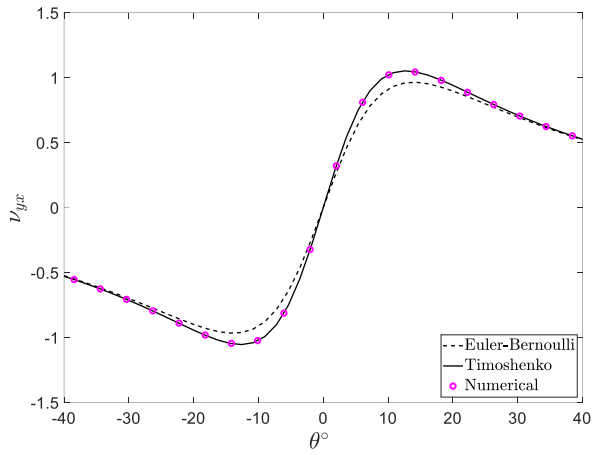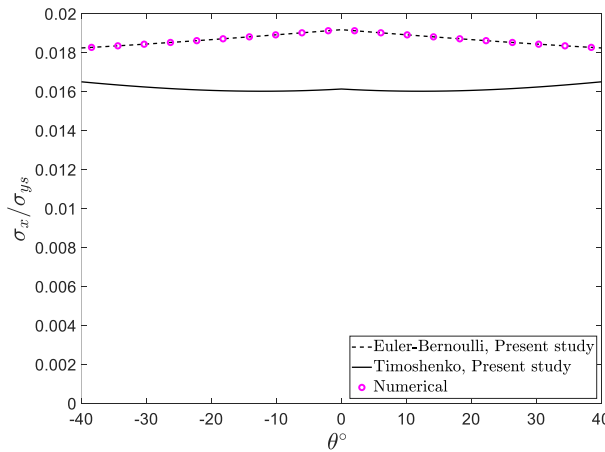
12
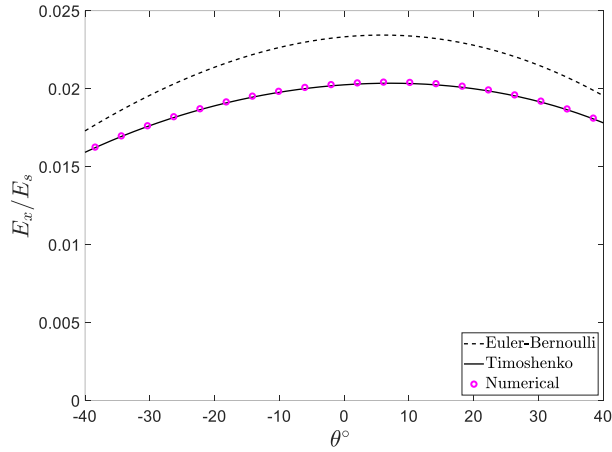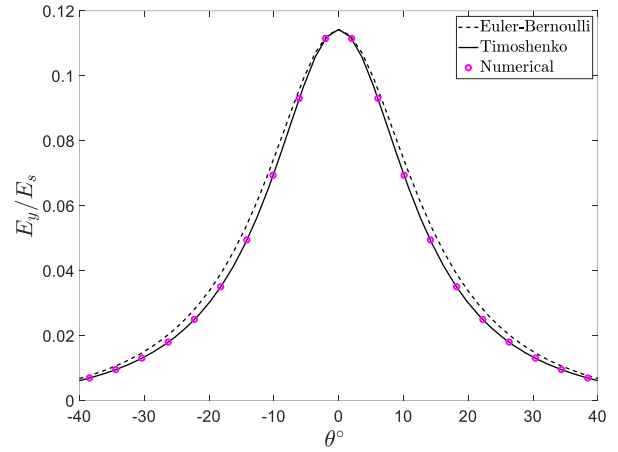
(a)　　　　　　　　　　　　**(b)**
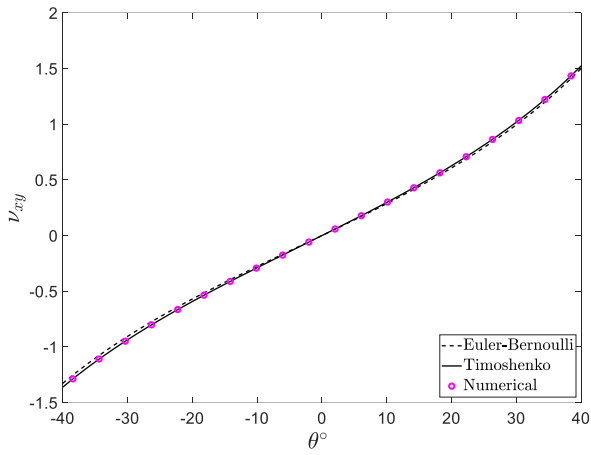
(c)　　　　　　　　　　　　**(d)**
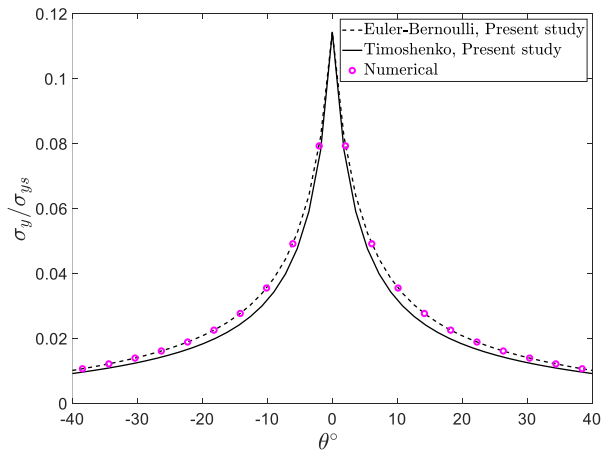
(e)　　　　　　　　　　　　**(f)**

Figure 3: Comparison of (a) E_x, (b) E_y, (c) ν_{xy}, (d) ν_{yx}, (e) σ_x, and (f) σ_y between the numerical and analytical results for $s = \frac{W - H\tan(\theta) - h}{2}$

The final interesting point would be the buckling stress and its comparison to yield strength and to know which of the two is the governing mechanism in collapsing of the lattice structure under compression. The results for buckling stress in the X and Y directions for W=0.014 m, H= 0.00667 m, b=0.004 m, and t=0.0008 m is presented in Figure 4. If the values are normalized with respect to σ_{ys} of polymers (which is in order of tens of MPa) and metals (which is in order of hundreds of MPa), it can be seen that the buckling stress lays in the range of ~0.001 and ~0.01,. Therefore, buckling stress values are comparable to yield stress values. As a result, depending on the situation, either yielding or buckling can play the main role in the collapse of the lattice structure in compression.
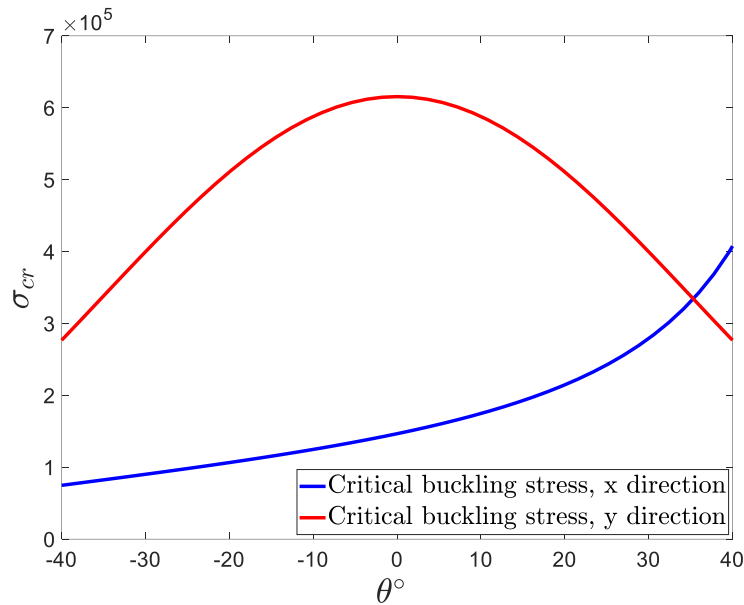

Figure 4: Variation of buckling stresses in the X and Y directions with respect to θ

4. Conclusions

The goal of this study was to find out if the analytical relationships obtained in the literature for $\theta > 0$ are also applicable to 2D-reentrant structures. Therefore, this study focused on unit cells with a wide range of internal angles from very negative to very positive. For this aim, new analytical relationships were obtained for hexagonal honeycombs with possible negativity in the internal angle θ in mind. Numerical analyses based on finite element (FE) method were also implemented to validate and evaluate the analytical solutions. The results showed that, as compared to analytical formulas

presented in the literature, the analytical solutions derived in this work give the most accurate results for elastic modulus, Poisson's ratio, and yield stress. Moreover, some of the formulas for yield stress available in the literature fail to be valid for negative ranges of internal angle (i.e. for auxetics). However, the yield stress results of the current study demonstrated good overlapping with numerical results in both the negative and positive domains of θ.

References

1. Hedayati, R. and S. Lakshmanan, *Pneumatically-Actuated Acoustic Metamaterials Based on Helmholtz Resonators.* Materials, 2020. **13**(6): p. 1456.
2. Nicolaou, Z.G. and A.E. Motter, *Mechanical metamaterials with negative compressibility transitions.* Nature materials, 2012. **11**(7): p. 608-613.
3. Critchley, R., I. Corni, J.A. Wharton, F.C. Walsh, R.J. Wood, and K.R. Stokes, *The Preparation of Auxetic Foams by Three-D imensional Printing and Their Characteristics.* Advanced Engineering Materials, 2013. **15**(10): p. 980-985.
4. Rafsanjani, A. and D. Pasini, *Bistable auxetic mechanical metamaterials inspired by ancient geometric motifs.* Extreme Mechanics Letters, 2016. **9**: p. 291-296.
5. Kolken, H.M. and A. Zadpoor, *Auxetic mechanical metamaterials.* RSC advances, 2017. **7**(9): p. 5111-5129.
6. Hedayati, R., S.J. Salami, Y. Li, M. Sadighi, and A. Zadpoor, *Semianalytical geometry-property relationships for some generalized classes of pentamodelike additively manufactured mechanical metamaterials.* Physical Review Applied, 2019. **11**(3): p. 034057.
7. Mohammadi, K., M. Movahhedy, I. Shishkovsky, and R. Hedayati, *Hybrid anisotropic pentamode mechanical metamaterial produced by additive manufacturing technique* Applied Physics Letters, 2020. **117**(6): p. 061901.
8. Hedayati, R., M. Mirzaali, L. Vergani, and A. Zadpoor, *Action-at-a-distance metamaterials: Distributed local actuation through far-field global forces.* APL Materials, 2018. **6**(3): p. 036101.
9. Sedal, A., M. Fisher, J. Bishop-Moser, A. Wineman, and S. Kota. *Auxetic Sleeves for Soft Actuators with Kinematically Varied Surfaces.* in *2018 IEEE/RSJ International Conference on Intelligent Robots and Systems (IROS).* 2018. IEEE.
10. Pan, Q., S. Chen, F. Chen, and X. Zhu, *Programmable soft bending actuators with auxetic metamaterials.* Science China Technological Sciences, 2020: p. 1-9.
11. Evans, K.E. and A. Alderson, *Auxetic materials: functional materials and structures from lateral thinking!* Advanced materials, 2000. **12**(9): p. 617-628.
12. Wang, H., Z. Lu, Z. Yang, and X. Li, *A novel re-entrant auxetic honeycomb with enhanced in-plane impact resistance.* Composite Structures, 2019. **208**: p. 758-770.

13. Wang, Z. and H. Hu, *Auxetic materials and their potential applications in textiles.* Textile Research Journal, 2014. **84**(15): p. 1600-1611.

14. Slann, A., W. White, F. Scarpa, K. Boba, and I. Farrow, *Cellular plates with auxetic rectangular perforations.* physica status solidi (b), 2015. **252**(7): p. 1533-1539.

15. Alderson, A., K.L. Alderson, D. Attard, K.E. Evans, R. Gatt, J.N. Grima, W. Miller, N. Ravirala, C. Smith, and K. Zied, *Elastic constants of 3-, 4-and 6-connected chiral and anti-chiral honeycombs subject to uniaxial in-plane loading.* Composites Science and Technology, 2010. **70**(7): p. 1042-1048.

16. Lorato, A., P. Innocenti, F. Scarpa, A. Alderson, K. Alderson, K. Zied, N. Ravirala, W. Miller, C. Smith, and K. Evans, *The transverse elastic properties of chiral honeycombs.* Composites Science and Technology, 2010. **70**(7): p. 1057-1063.

17. Huang, H.H., B.L. Wong, and Y.C. Chou, *Design and properties of 3D-printed chiral auxetic metamaterials by reconfigurable connections.* physica status solidi (b), 2016. **253**(8): p. 1557-1564.

18. Lv, C., D. Krishnaraju, G. Konjevod, H. Yu, and H. Jiang, *Origami based mechanical metamaterials.* Scientific reports, 2014. **4**: p. 5979.

19. Kamrava, S., D. Mousanezhad, H. Ebrahimi, R. Ghosh, and A. Vaziri, *Origami-based cellular metamaterial with auxetic, bistable, and self-locking properties.* Scientific reports, 2017. **7**(1): p. 1-9.

20. Whitty, J., F. Nazare, and A. Alderson, *Modelling the effects of density variations on the in-plane Poisson's ratios and Young's moduli of periodic conventional and re-entrant honeycombs-Part 1: Rib thickness variations.* Cellular Polymers, 2002. **21**(2): p. 69-98.

21. Wan, H., H. Ohtaki, S. Kotosaka, and G. Hu, *A study of negative Poisson's ratios in auxetic honeycombs based on a large deflection model.* European Journal of Mechanics-A/Solids, 2004. **23**(1): p. 95-106.

22. Fu, M., O. Xu, L. Hu, and T. Yu, *Nonlinear shear modulus of re-entrant hexagonal honeycombs under large deformation.* International Journal of Solids and Structures, 2016. **80**: p. 284-296.

23. Ghavidelnia, N., S. Jedari Salami, and R. Hedayati, *Analytical relationships for yield stress of five mechanical meta-biomaterials.* Mechanics Based Design of Structures and Machines, 2020: p. 1-23.

24. Hedayati, R., M. Sadighi, M. Mohammadi Aghdam, and A.A. Zadpoor, *Mechanical properties of additively manufactured thick honeycombs.* Materials, 2016. **9**(8): p. 613.

25. Gibson, L.J. and M.F. Ashby, *Cellular solids: structure and properties.* 1999: Cambridge university press.

26. Masters, I. and K. Evans, *Models for the elastic deformation of honeycombs.* Composite structures, 1996. **35**(4): p. 403-422.

27. Mirzaali, M., R. Hedayati, P. Vena, L. Vergani, M. Strano, and A. Zadpoor, *Rational design of soft mechanical metamaterials: Independent tailoring of elastic properties with randomness.* Applied Physics Letters, 2017. **111**(5): p. 051903.